The influence of geology on a simulated rockburst

by N. Reddy* and S.M. Spottiswoode†

Synopsis

The influence of local geology and rock mass characteristics on deformations during a rockburst caused by a controlled blast was studied. This was done by means of visual examination, mapping and photography both before and after the blast. We found that the ejected material was bounded mostly by fractures associated with the bow-wave fracturing and bedding surfaces and that existed prior to the blast. Most of the damage was caused by shake-out. This information is important input for the design of rockburst resistant support systems under conditions of moderate stress.

Introduction

Although many rockbursts have been intensely studied, there are many unanswered questions concerning mechanisms of rockburst damage. Durrheim *et al.*[1] found that the location and severity of rockburst damage is strongly influenced by, amongst other factors, local rock conditions. Spottiswoode *et al.*[2] found that an increase in ground velocities are expected in stopes surrounded by more intense fracturing.

A simulated rockburst experiment was performed in an underground mine tunnel. Details of this project are provided in the overview paper by Hagan *et al.*[3]. The purpose was to create a controlled seismic event, which could be extensively monitored (Milev *et al.*[4]), to induce damage in a tunnel and to study this damage. The experiment used blasts set in five boreholes at about 8 m from the tunnel to generate the incident seismic waves that would damage the sidewall. The blast gases ejected the tamping and voided through the boreholes without causing gas-driven fractures or block ejection from the tunnel sidewall.

Peak particle velocities of up to 3.3 m/s were measured on the sidewall of the tunnel and the event was recorded with a Magnitude M = 1.3 by the mine network[4]. The influence of local geology and rock mass characteristics on rockburst damage was investigated in this work.

The experiment site was situated at Kopanang Mine (Vaal Reefs No. 9 shaft), Vaal River Operations in the Klerksdorp goldfield. The experiment was conducted in the disused 53 BW23 crosscut south 1600 m below surface. The maximum field stress estimated from modelling was 50 MPa.

The tunnel was supported with shepherd's crooks, mesh and lace. In order to make the damage more visible, the mesh and lace were removed along the side of the tunnel closest to the blast. The relationship between the support and the damage is reported by Haile and le Bron[7] in an accompanying paper.

Instrumentation and monitoring

The site was examined before and after the blast. The following was conducted before the blast:

- Mapping of the crosscut to determine primary and secondary structures
- Borehole petroscopy to determine the positions of existing discontinuities
- Photography of the crosscut sidewall to provide a visual record
- Installation of extensometers.

The sidewall was whitewashed after examination and prior to the blast. The following was conducted after the blast:

- Borehole petroscopy
- Photography of the sidewall
- Measurement of ejected sidewall blocks due to the blast
- Examination of the sidewall and hangingwall
- Mapping of newly formed fractures
- Extensometer measurements
- Borehole video filming of the shotholes.

* *P.O. Box 947, Banbury 2164, South Africa.*

† *CSIR: Division of Mining Technology, Auckland Park, South Africa*

 SA ISSN 0038–223X/3.00 + 0.00. Paper received Feb. 2001; revised paper received Aug. 2001.

Figure 1 illustrates the tunnel with location of the extensometer holes closest to the blast and shows representative orientations of discontinuities. Positions along the tunnel were measured from a datum using a reference tape. as marked in Figure 1. All references to distances along the tunnel in this text are with respect to this datum.

Pre-blast observations

Local geology

The lithologies in the tunnel comprise argillaceous quartzites of the Strathmore formation known locally as the MB2. The quartzites are grey and argillaceous. Black, laterally impersistent argillite lenses occur locally within the quartzite.

A north-south trending normal fault, dipping 72° to the east, is shown in Figure 1 at –15 m. The above-mentioned quartzites are in the hangingwall of the Vaal Reef as the fault throws down to the east by approximately 100 m. Mining occurs to the west of the fault. There is evidence of limited strike slip movement on the fault.

Bedding

Bedding strike varies from NE to NNE southeasterly along the tunnel (Figure 2). Dip of beds varies from 55° at 8 m to 30° at 28 m. Steeper dips closer to the fault are probably due to drag on the fault.

Bedding surfaces are defined by thin, less than 5 mm, argillite partings or by changes in grain size. The beds are coarse at the bottom becoming finer upwards. Bedding surfaces are generally welded and closed. Movement along bedding surfaces was detected closer to the fault probably because of the drag mentioned earlier.

Figure 3 shows the variation of bedding spacing with distance along the tunnel. Bedding spacing varies between 150 and 300 mm along the first 10 m of the tunnel, after which it increased to a maximum 600 mm.

Jointing

The major joint trend strikes NNE sub-parallel to the normal fault with moderate dips to the W (Figure 2). Joint spacing varies from 0.5–3.0 m. All joints are closed with a hard khaki or dark green infilling, probably chlorite. They are generally planar with slight waviness near bedding surfaces.

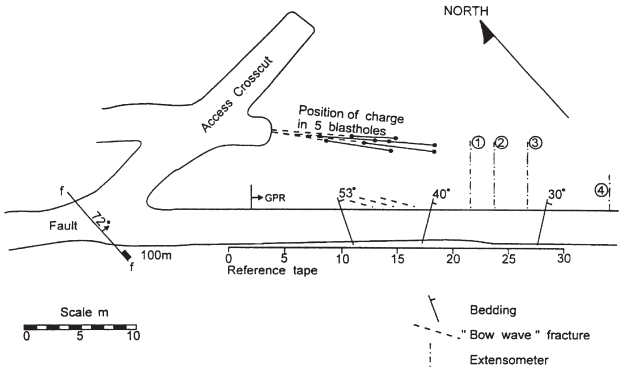

Figure 1—Geometry of the testing site. Extensometer boreholes 5 and 6 were off to the right of the picture

Micro-displacements of up to 30 mm were measured on joints cutting through beds. Conversely, joints were offset by up to 10 mm by bedding planes. These effects were more pronounced in the vicinity of the fault.

Fracturing

Bow-wave fractures associated with the original development trend NNW on the NE sidewall and dip at 85°–90° (Figure 2). They define angles of between 10° and 20° with the sidewall and are generally open (up to 2 mm), clean, and moderately smooth. Within the tunnel sidewall, bow-wave fractures turn towards being parallel to the tunnel sidewall and define wedges. Over the distance measured (along the reference tape), fracture spacing at first decreases until approximately 15 m after which they open up (Figure 4).

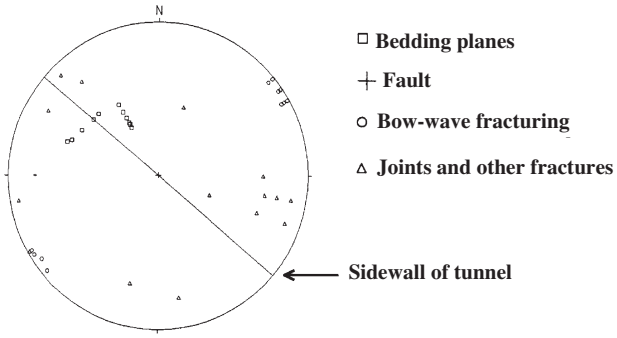

Figure 2—Lower hemisphere, Schmidt stereoplot of mapping

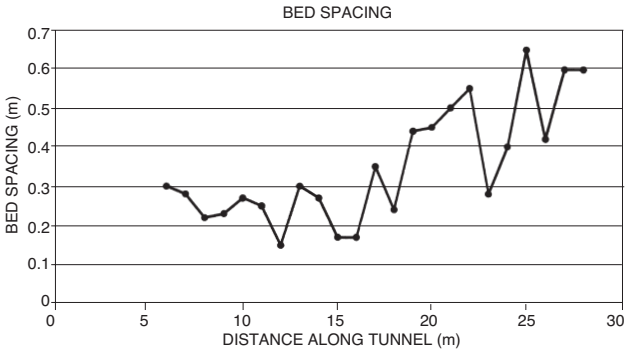

Figure 3-Bed spacing along the tunnel

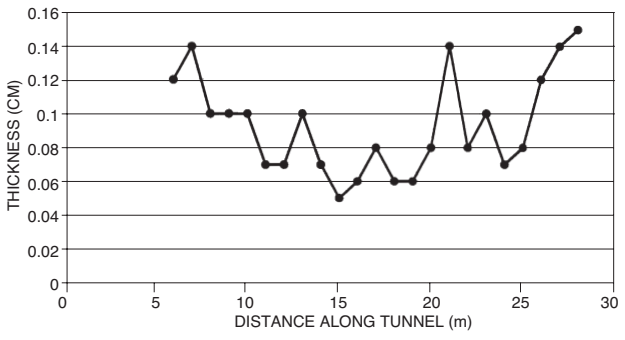

Figure 4—Fracture spaing along the tunnel

The degree of fracturing was commensurate with the estimated field stress of 50 MPa. Tunnels that are, or have been, subjected to field stresses well in excess of 50†MPa show tunnel-parallel fracturing and massive sidewall movement that is exacerbated by strong ground motion.

Extensometer measurements

Six holes installed with extensometer anchors were drilled between 22 m and 43 m. They were designed to measure dilation at the surface of the tunnel and at intervals into the rock. Anchors were installed from the beginning of the hole up to 6 m into the sidewall. Initial anchor positions were recorded. Holes 1, 2, 3 and 4 are shown in Figure 1. Holes 5 and 6 were located at 38 m and 42 m and to retain greater graphic detail around the area of greatest interest, they are not shown in Figure 1. These holes were mapped using a petroscope before and after the blast.

Post-blast observations

Block size analysis

The dimensions of all ejected blocks with lengths greater than 30 cm were measured as they lay on the tunnel floor. The limit of 30 cm was chosen to make the measurement by hand tractable and also to avoid moving large blocks to expose smaller blocks buried underneath them. Unfortunately, we could not judge exactly where each block came from. We measured each block in terms of dimensions of the smallest parallelepiped surrounding that block, with length >= breadth >= thickness. If the original whitewash painted on the sidewall was visible, it was most often either on the top or the bottom of each block, indicating that the thickness was controlled by the bow-wave fractures as they terminated on the tunnel sidewall.

The damaged zone defined by the volume of ejected blocks in Figure 5 lies between approximately 8 m and 24 m along the tunnel. The most intense damage occurred between 9 and 19 m, corresponding exactly to the position of the explosives. This area was within 10 m of the centre of the blast and, from Milev *et al.* (Figure 8)[4], was subject to peak velocity of 1.5 m/s and more. The area of less damage from 19 to 28 m was ahead of the position of the blast holes and subject to velocities in excess of 0.5 m/s. No damage was observed on the tunnel sidewall along the section where the holes were tamped. Hildyard and Miliev7 explained this asymmetry in terms of the direction of blast propagation. Very little damage was observed on the opposite wall.

It can be seen in Figure 6 that neither the breadth nor the thickness of the ejected blocks correlated with their length. A similar analysis shows that the breadths and length also do not correlate with one another. The size of the measured blocks appeared to have been controlled as follows.

- Thickness: 0.1 m to 0.2 m, similar to the spacing of the bow-wave fractures
- Breadth: 0.2 m to 0.5 m, similar to the bedding-plane thickness
- Length: 0.4 m to 0.8 m. Either support spacing or excessive slenderness probably limited the length.

The blocks that we measured along the 10.4 m of most intense damage had a total volume of 0.75 m^3 and area (length times breadth) of 4.77 m^2, with average thickness over this area of 0.16 m. As the tunnel height was about 3 m, the larger ejected blocks initially covered about 3.2% of the area of the sidewall. As shown in Figures 8 and 9, the actual area of ejection was much more than 3% of the tunnel sidewall, perhaps about 30%. The far more numerous smaller blocks that we did not measure must have accounted for most of the bulk of the area, if not the volume, of ejected material.

The volume (V) distribution of the blocks is shown in Figure 7. There is a clear kink at V = 0.02m^3 in the distri-

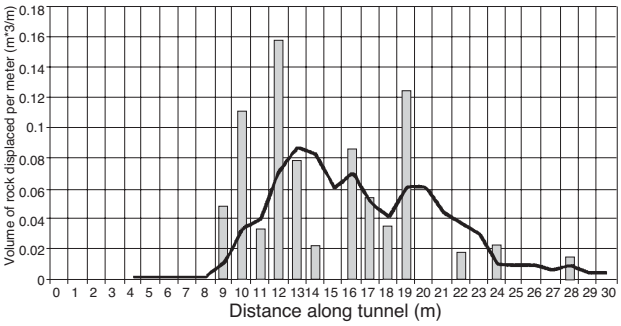

Figure 5—Ejected blocks along the runnel per metre (bars) and smoothed profile (line)

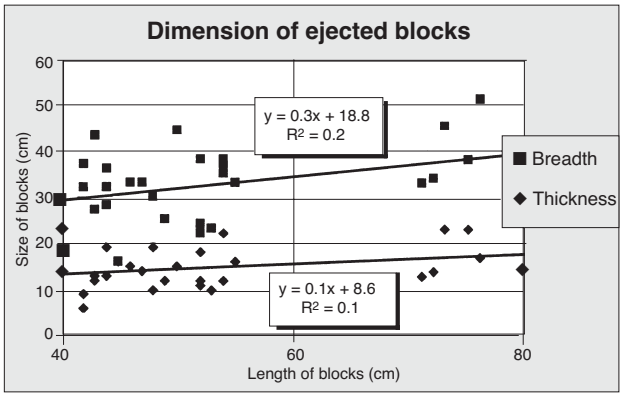

Figure 6—Breadth and thickness of ejected blocks as functions of their length

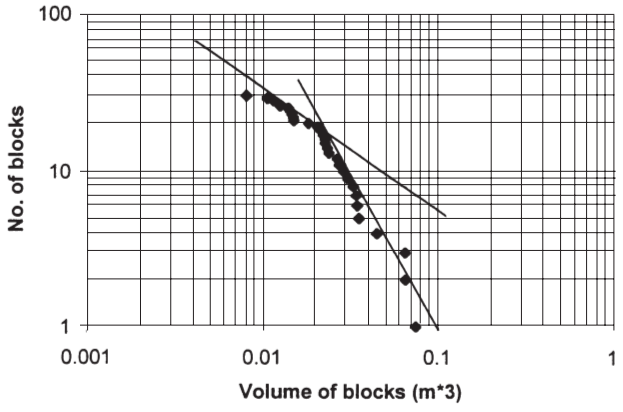

Figure 7— Distribution of block volumes. Lines indicate power-law behaviour

bution, showing different power-law scaling for larger and smaller blocks. Smaller blocks scale as $N \sim V^{-1}$ and larger blocks scale as $N \sim V^{-2}$.

The region of application of the $N \sim V^{-1}$ power-law behaviour is only a factor of two, being terminated at the lower value by our choice of minimum length of 400 mm. 10 blocks had volumes between 0.01 and 0.02 m^3. If the $N \sim V^{-1}$ were to persist, then 20 blocks would have sizes between 0.005 and 0.01 m^3, 40 blocks between 0.0025 and 0.005 m^3 and so on. Each factor of two would contribute equal volumes that, if allowed to continue to zero size, would result in an infinite pile of dust. On the other hand, a similar graph of the distribution of areas (A = length times width) scales as $N \sim A^{-1.5}$. In this case, smaller sizes contribute more with all blocks for each factor of ten decrease in size contributing about three times the total area (A) of all larger blocks. A coverage of 30% could be achieved if $N \sim A^{-1.5}$ persisted for smaller blocks and particles a hundred fold smaller than the smallest that we measured, namely down to a size of a few mm in length.

Petroscopy

Holes drilled perpendicular to the sidewall were examined with a petroscope to a depth of 3 m. New fractures were formed within the first metre. They were less than 1 mm wide, clean and wavy. The strike of the fractures was 80° to 90° to the borehole. The new fractures are regarded as tensile.

Extensometer measurements

Dilation measurements for the six extensometer stations are given in Table I. Maximum dilation measured at the surface was 7 mm, diminishing with distance from the damaged area. As no sidewall fracturing was seen at depth beyond 0.5 m in any of the holes before the blast, we expected that the measuring points would not move closer to one another. In other words, the distance of each point from the reference point on the opposite sidewall should not be more than the distance for any shallower point in the same borehole. In Table I we have indicated with '?' measurements that exceeded shallower readings by more than 1mm. The extreme accelerations very close to the blast might have moved the anchors and the design of the in-hole anchors would have favoured inward movements.

Sidewall examination

The sidewall was examined and various observations were made. Smaller zones of ejection were irregular in outline and generally defined by new fractures unless near bedding planes. Larger zones were defined by pre-existing (bow-wave) fractures along their SE extremities and by new fractures on their NW extremities (Figure 8).

Ejected blocks from the sidewall are controlled to a certain extent by bow-wave fracturing and bedding spacing. Figure 9 illustrates the relationship between bedding surfaces and the area of ejection, as was also suggested from the blocks sizes (section 4.1 above). The area of ejection is bounded on some sides by bedding. The size of ejected blocks will therefore be controlled by the occurrence of bedding and hence bedding spacing. Jointing plays a very minor role. No failure of sidewall support units was found, although ejection of rock occurred around some of the support units.

Inspection of newly-exposed sidewall formed after the blast had the following characteristics:

The majority of fractures were terminated at one or both edges by bedding surfaces and to a lesser degree by pre-existing discontinuities. Some fractures emanated from sidewall support units. Most fractures terminated against other fractures, with only a few ending in solid rock. Fracture openings varied from 0,2–3,0 mm. The majority of fractures were irregular.

The damage to the sidewall was thus largely controlled by pre-existing discontinuities and was therefore mostly due shake out damage. In addition, because the tunnel was not

Table I

Extensometer closure measurements. Spurious measurements, exceeding bymore than 1 mm any shallower measurement withing the same hole, are marked with '?'

	6 m	5 m	4 m	3 m	2.5 m	2 m	1.5 m	1 m	0.5 m	0 m
Ex 1	6?	10?	3	5?		2		3		5
Ex 2	5?	0	4	3	5	5	7?	4	4	7
Ex 3	2?	1	9?	0		0		0		4
Ex 4						4?		0	3	3
Ex 5						1		0	3	0
Ex 6						0		0		0

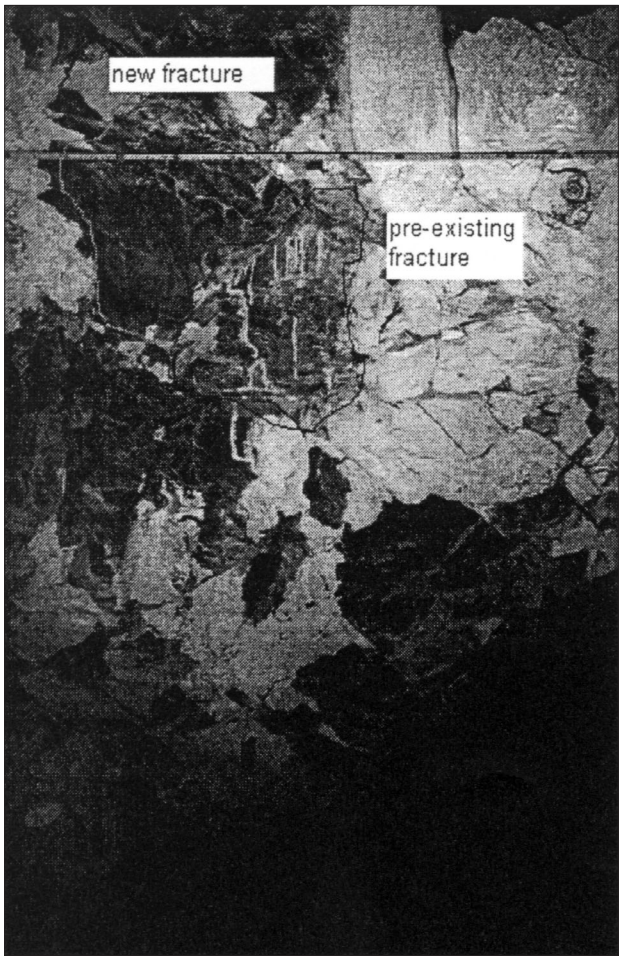

Figure 8—Photograph of an area of ejection

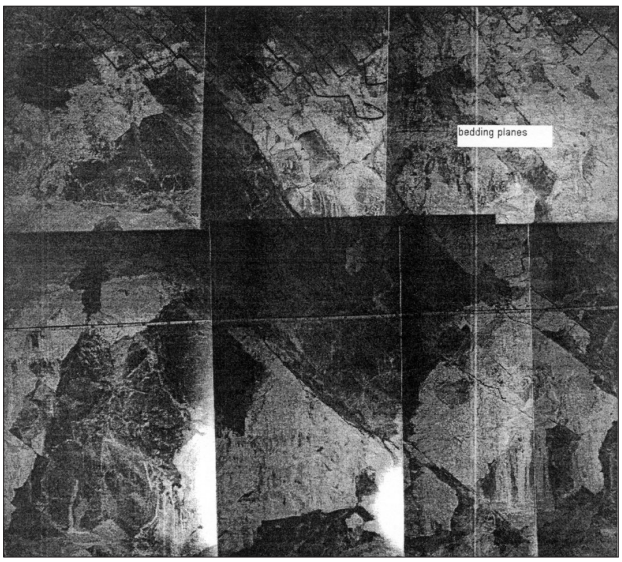

Figure 9. Photo-mosaic showing area of ejection and bedding planes. Bedding dips down to the right

surrounded by a thick fractured zone, opportunities for dilation were limited.

Hangingwall and opposite sidewall damage

The hangingwall was wire-meshed and laced and a thorough examination was therefore not possible. A cursory examination was conducted to determine the location of fallout blocks and their dimensions.

Ejected blocks occurred between 12 and 22 m along the tunnel with the largest block being 0.1 m^2 in area. Sixty three percent of the ejected blocks were bedding related while the rest were fracture- or joint related. Ejection of blocks is considered to be a function of the loosest blocks being shaken out along pre-existing discontinuities. The relative absence of damage to the hangingwall compared to the sidewall may give an indication of the direction of the seismic wave source. No damage was recorded on the opposite sidewall. Locally, loose blocks were found resting against the wire mesh.

Damage around the blast holes

After the blast all five blast holes were examined using a borehole video camera. The examination showed that a large vertical crack had formed connecting all boreholes, most probably along almost their entire length. The crack has a 'wavy' shape with the opening decreasing from the collar (left frame of Figure 10) of the hole towards the toe (right frame in Figure 10).

The edges of the crack near the mouth of the hole were rounded, presumably through sandblasting by the violent ejection of the tamping and the material gouged out of the crack. The right-most frame shows a more complex pattern of fractures. As the distance of the camera to the borehole wall varied, the typical grain size of 1mm was used as a crude scale. From this, the crack opening appeared to be between 1 and 2 mm.

Influence of geology on tunnel damage

Ejected block dimensions were strongly controlled by prior fracturing , with the thickness of blocks being controlled by the bow-wave fractures and the breadth of the blocks controlled by bed spacing.. Pre-existing discontinuities therefore influence block dimensions to a certain extent. Higher densities of pre-existing discontinuities may lead to higher volumes of ejected material.

Rare occurrences of mirror zone fractures were seen. These fractures suggest dynamic fracturing probably as a result of the blast. This type of fracture may occur where blast waves are the strongest.

The argillaceous quartzites are relatively weak and three tests revealed an average uniaxial strength of 129 MPa. Argillaceous quartzites exhibit a lower degree of fracturing than siliceous quartzites, Daehnke et al.[5]. Rock type and strength will therefore influence the amount of damage and ejected rock.

Conclusions

Prior fractures of geological and mining origin appeared to have influenced the damage in the following ways:

- Joints were much more widely spaced than the mining-induced bow-wave fractures and therefore their influence on the burst material was small. It is also likely that jointing will only play a small role in fragmentation at all deep sites. It should be remembered, however, that jointing remains an important consideration in creating individual key blocks
- If any bedding surfaces are open, then they are most likely to be mobilized during a rockburst and control the shape and size of the burst material
- Mining-induced fractures had the largest influence at this particular site because of their intensity. Similarly,

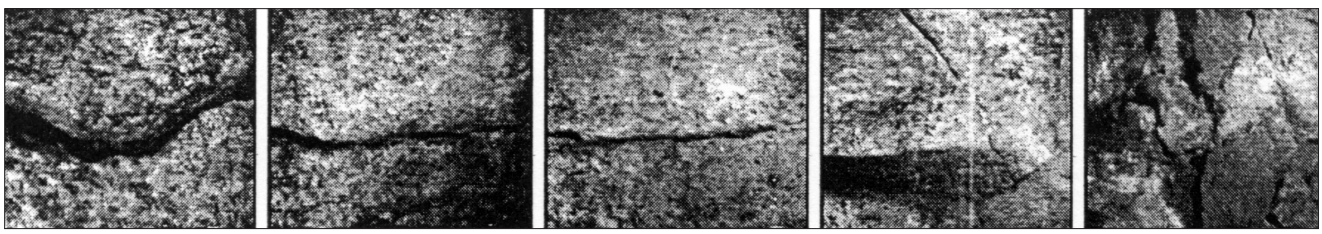

Figure 10—Sequence of photograph showing the shape of the crack running through the charge holes. Deeper from the left to right

more intense induced fracturing would lead to greater opportunity for rock mobilization and would require containment support for control
- ➤ Geological weaknesses could play a larger role at shallower sites where mining induced fractures are not important.

Acknowledgement

This work was sponsored by SIMRAC under project GAP530. Thanks to Mark Grave for providing the petroscope and extensometer data, Alex Milev for considerable assistance in preparing the manuscript and Terry Hagan and an anonymous reviewer for valuable advice.

References

1. Durrheim, R.J., Roberts, M.K.C., Haile, A.T., Hagan, T.O., Jager, A.J., Handley, M.F., Spottiswoode, S.M., and Ortlepp, W.D. Factors influencing the severity of rockburst damage in South African gold mines. *Journal of South African Institute for Mining and Metallurgy* vol. 98, no. 2. 1998. pp. 53–57.
2. Spottiswoode, S.M., Durrheim, R.J., Vakalisa, B. and Milev, A.M. Influence of fracturing and support on the site response in deep tabular stopes. *SARES 97. Proceedings 1st South African Rock Engineering Symposium*, Johannesburg. Gurtunca, R.G. and T.O. Hagan (ed.), 1997, pp. 62–68.
3. Hagan, T.O., Milev, A.M., Spottiswoode, S.M., Hildyard, M.W., Grodner, M., Rorke, A.J., Finnie, G.J., Reddy, N., Haile, A.T., Le Bron, K.B., and Grave. D.M. Simulated rockburst experiment–an overview. *The Journal of The South African Institute of Mining and Metallurgy*, 2001, submitted.
4. Milev, A.M., Spottiswoode, S.M., Rorke, A.J., and Finnie, G.J. Seismic monitoring of a simulated rockburst on a wall of an underground tunnel. *The Journal of The South African Institute of Mining and Metallurgy*, 2001, submitted.
5. Grave, M.D. The extensometer results of sidewall monitoring of 53–34 crosscutat Vaal Reefs 9 Shaft following the simulated rockburst. *Internal report. CSIR–Miningtek*, 1998, Johannesburg. 5 p.
6. Daehnke, A., Andersen, L.M., de Beer, D., Esterhuizen, G.S., Glisson, F.J., Jaku, E.P., Kuijpers, J.S., Kullmann, D.H., Peake, A.V., Piper, P.S., Quaye, G.B., Reddy, N., Roberts, M.K.C., Schweitzer, J.K., and Stewart, R.D., Stope face support systems. *SIMRAC Final Project Report GAP* 330. Pretoria: Department of Minerals and Energy, 1998. 407 p.
7. Haile A. T. and le Bron K. B. Simulated rockburst experiment ñ evaluation of rock bolt reinforcement performance. *J. of South African Ins. of Mining and Metallurgy*, submitted for publication. 2001.
8. Hildyard, M. W., and Milev, A. M. Simulated rockburst experiment: Development of a numerical model for seismic wave propagation from the blast, forward analysis. *J. of South African Ins. of Mining and Metallurgy*, submitted for publication. 2001. ◆